TARGET DETECTION IN HYPERSPECTRAL MINERAL DATA USING WAVELET ANALYSIS

Michael Mitchley[1]*, Michael Sears*[1] *and Steven Damelin*[2,3]

[1]School of Computer Science
University of the Witwatersrand
Johannesburg, South Africa

[2]School of Computational and Applied Mathematics
University of the Witwatersrand
Johannesburg, South Africa

[3]Department of Mathematical Science,
Georgia Southern University, Statesboro
GA 30460, USA

ABSTRACT

A method for the automatic supervised detection of multiple mineral targets in hyperspectral mineral data is presented in this paper. The method makes use of wavelet analysis, wavelet-based denoising using thresholding of wavelet detail coefficients, and feature reduction based on sequential forward selection, which utilises an extension of receiver operating characteristic curves to fuzzy set membership in order to measure discriminating capability.

The method is shown to run in time linear to the number of hyperspectral bands, per pixel. Furthermore, an extension of this method to linear unmixing is presented, based on minimising the least-squares error between abundance estimates and actual spectra by varying a thresholding parameter to eliminate outliers and imposing a sum-to-one constraint on the abundances.

Index Terms— wavelet transforms, target detection, feature extraction

1. INTRODUCTION

Hyperspectral imagery is a recently developed field of remote sensing that yields far richer data than traditional colour or multispectral imagery. However, this data comes at the price of high dimensionality, causing greatly increased difficulty in classification. Further challenges are encountered when hyperspectral imagery is used in mineral applications, such as nonlinear mixing effects.

The Hyperspectral Core Imager (HCI) is a device owned by AngloGold-Ashanti used for obtaining hyperspectral scans of mining cores. Cylindrical mining cores are cut in half, and the flat surface scanned by the HCI to obtain a continuous spectrum ranging from visible light to the shortwave infra-red for each pixel. Endmember extraction is used to reduce the dimension of the spectral vector associated with each pixel, and the reduced feature set is clustered using self-organising memory.

Two problems are encountered: firstly, the process is slow, and it was found that pixels clustered together often had sufficiently different spectral signatures to be considered different minerals. This implies the need for a system that is both computationally efficient and accurate. The second problem leads to the idea of target detection. At present, it is not possible to automatically discover the mineral group associated with each cluster. It is necessary for a spectral geologist to examine the spectral signatures found in each cluster to identify each mineral [1].

Thus, a problem of target detection can be defined in the following sense. Given the hyperspectral data of a core scan, and a number of target minerals to find within the core, is it possible to detect instances of the targets in the data in an accurate, quantitative and computationally efficient manner? Furthermore, can this method be extended to provide an unmixing of the hyperspectral data into abundances of each target?

2. METHODOLOGY

The target detection method presented is made up of several distinct stages, and will thus be referred to as the multistage method in this paper. To outline the method briefly, the hyperspectral data is subjected to an orthonormal wavelet transform (specifically, a D8 wavelet is used) in the spectral domain, and denoised using wavelet thresholding. The denoised wavelet coefficients are then reduced to a small subset of features using the results of a supervised feature reduction method known as Sequential Forward Selection. This reduced feature set is of much lower dimensionality, and an accurate distance measure can be taken for each target. This distance measure is measured against a tolerance found automatically by the SFS method to obtain a quantitative target detection map.

Finding the SFS feature subset and tolerance for each target constitute the preprocessing stage of the multistage method. The processing of the hyperspectral data and generation of the target detection map make up the processing stage. A post-processing step

The authors would like to thank AngloGold Ashanti as well as the Anglo Technical Division, Geoscience Research Group and in particular Phil Harris, for providing data for this project. Steven Damelin acknowledges support from the NSF, EPSRC, UAIM (GSU) and Wits.

imposes a sum-to-one constraint on the target detection map to generate an unmixed abundance map that minimises the least-squares error.

The target detection scheme (pre-processing and processing stages) is based on that outlined in [2] and [3], although a number of key modifications should be highlighted. Firstly, both papers tackle the problem of binary classification, where the two end classes are well-defined. Secondly, in our scheme the noisy hyperspectral data is denoised using wavelet thresholding techniques. Finally, the Receiver Operating Characteristic (ROC) curves are created in a fuzzy way to facilitate quantitative mapping.

2.1. Pre-Processing

Some pre-processing must take place before the method can be applied to hyperspectral core images. It is necessary to compute features to extract, and the tolerances to use in the distance measure. This is done through a supervised feature extraction method called Sequential Forward Selection (SFS). SFS relies on being able to measure the discriminating capability of a subset of features. In this application, this is accomplished with ROC curves, as it was in [2], [3] and [4]. The SFS implementation used is that of [4]. While this method is suboptimal, an exhaustive search of possible feature subsets would be prohibitively expensive, taking roughly $O(n^m)$ time, where n is the number of features to choose from, and m is the maximum size of the feature subset.

A training set of linear mixtures of seven target minerals was created to train the SFS method. The target minerals chosen for this study were chlorite, chloritoid, a flat spectrum, pyrophyllite, quartz and two kinds of sericite. To keep the training set at a reasonable size, ten hyperspectral samples of each target were mixed pairwise, and half of the resulting mixtures were chosen as the training elements. The other half were reserved for a testing set. While the minerals in a rock are intimately mixed, resulting in nonlinear mixtures, it was assumed that linear mixing effects dominate in the fine spatial resolution of the HCI.

Information was appended to the training set, showing the abundance of each target in the linear mixture. We can alternatively think of this as fuzzy set membership into each target class. The SFS method was then run for each target. The classifier in the ROC method was modified to take the Euclidean distance d of the subset of training element features and compare this to some tolerance α. The resulting match M was given by

$$M = \begin{cases} 0 & \text{if } d \geq \alpha \\ 1 - \frac{d}{\alpha} & \text{otherwise} \end{cases} \quad (1)$$

The match M is fuzzy, and so sensitivity and specificity across the training set were defined in a fuzzy manner. Agreements between the match M and the true value were added to the true positive and true negative counts, while the area of disagreement was counted as either a false positive or a false negative, depending on the true value. By varying α, a ROC curve is obtained. The area under the curve (AUC) provides a measure of the discriminating capability of the feature subset. The tolerance giving the point on the curve furthest from the line of no discrimination (where specificity is equal to $1-$ sensitivity) is the tolerance giving the best results.

The SFS method iteratively grows an initially empty feature subset by adding to it the feature that would most increase its AUC, if any exist. The process is stopped when no more features can be added to the subset, or the maximum subset size m is reached. The time complexity of this method is quite high. However, it must be noted that preprocessing need only be performed once for each training and target set. As long as the training set is suitably representative of the data being processed, and we are looking for the same targets, we can reuse the feature subset and tolerance results for any number of data sets.

2.2. Processing

To minimise the effects of variation in reflectivity across the hyperspectral data set, all the data processed was normalised so that the spectral vector of each pixel was on the unit hypersphere (that is, having a norm of one). The data was then subjected to wavelet analysis, using a dyadic filter bank corresponding to the Daubechies D8 wavelet [5]. The level of decomposition was the maximum recommended by Matlab's wavelet toolbox. The use of wavelet analysis in hyperspectral data has been shown to produce better results for a variety of applications ([6] [7] [8] [2] [3] [9] [10]). For more background to wavelet techniques and signal processing, see Steven B. Damelin and Willard Miller, Topics in Applied Mathematics, Computer Vision, Imaging and Wavelets, Birkhauser (Benedetto eds.). The Universal Thresholding (UT) scheme of [11] was used to denoise the wavelet detail coefficients. A hard threshold was applied using a noise level estimate from the first level of decomposition.

The resulting denoised coefficients were then reduced to the required feature subset for each target, using the results from the SFS pre-processing stage. The Euclidean distance between the target features and pixel features was taken and a match was found using the optimal target tolerance and equation (1). This match is then the quantitative measure of that pixel's match to the target mineral. By repeating this process for each target and for every pixel, a quantitative target detection map is obtained.

The time complexity of the multistage method is easily shown. For each pixel, we consider a reduction from the original n spectral features to m wavelet features, for t targets. Wavelet analysis and denoising are performed in $O(n)$ time, since the wavelet is dyadic, and the threshold is a fixed, easily computed value. Reduction to the feature subset can be performed in $O(m)$ time, but this must be done for each target, resulting in a time complexity of $O(mt)$. The match can then be computed in $O(m)$ time per target, so finally the time complexity of the method is $O(n + mt)$ per pixel, where $m < n$. If m is chosen such that $mt < n$, we can simplify this complexity to $O(n)$ per pixel.

2.3. Post-Processing

We now consider an extension to the above multistage method. This extension aims to turn the quantitative target detection maps into abundance maps. If we make the assumption that the target detection matchings are potentially inaccurate, we consider a number of modifications that can be made at each pixel of the map. Firstly, if a particular target match is low in comparison to others at that pixel, we should consider zeroing it off as a false positive. This is especially the case with flat spectra. Secondly, if a particular target correlates poorly with neighbouring pixels, we should consider it an outlier. As the case of small abundance has been taken care of, we only consider the case of a potentially large abundance at the pixel, and small abundances at neighbouring pixels for this study. Thirdly, it may be necessary to multiply the matches of all the targets at a particular pixel by some value to grow or shrink them. We may wish to grow them if abundance values have been underestimated, or the presence of an unknown material has resulted in low matchings. We

may wish to shrink the matches if abundances have been overestimated.

Two constraints to bear in mind are the sum-to-one and nonnegativity constraints, which are required for the abundance ratios to have physical meaning. While the nonnegativity constraint is automatically satisfied by the matches (which are always between zero and one), it is necessary to impose the sum-to-one constraint. We thus define an optimisation problem. Given a match m_i for target t_i at a specific pixel with spectral vector A, and N_i defined as the maximum value of m_i across some defined neighbourhood of the pixel, we obtain the least-squares (LS) minimisation problem

$$\min_{\alpha,\beta} \left\| A - \beta \sum_i a_i t_i \right\|_2^2$$

where

$$a_i = \begin{cases} 0 & \text{if } m_i < \alpha \text{ or } N_i < \alpha \\ m_i & \text{otherwise} \end{cases} \quad (2)$$

subject to

$$\beta \sum_i a_i = 1$$

with i running across all t targets.

It can be shown that α can take on exactly $2t$ discrete values. We can then find β directly from the equality constraint. Thus, we can exhaustively search for optimal values of α and β to minimise the error and meet the sum-to-one constraint. Since the error must be computed for each possible tolerance α, the post-processing stage runs in time $O(nt^2)$ for each pixel. While this is more expensive than the multistage method, this should still acceptable, since typically $t << n$.

3. RESULTS

To demonstrate the effect of wavelet-based denoising on hyperspectral mineral data, four signals corresponding to the spectral signatures of three pure minerals (namely, chlorite, pyroxene and vesuvianite) were obtained from the website of the United States Geological (USG) survey digital spectral laboratory [12]. As this data was itself noisy, it was subjected to a smoothing filter, to obtain smooth clean signals representing ideal readings. These ideal readings were made noisy with Gaussian noise at predefined signal to noise ratios (SNR), and denoised with a variety of methods and parameters. It was found that single-level noise estimation combined with either hard UT thresholding or the SUREshrink method [13] produced the best results, summarised in table 1. While the SUREshrink method produced better results than UT, it must be mentioned that it is $O(n \log n)$, rather than $O(n)$, and its use would increase the complexity of the multistage method. As can be seen from the table, in almost all cases wavelet-based denoising leads to large improvements in signal quality. Pyroxene, the one signal not improved by denoising, was severely undersampled.

	soft SURE	hard UT
Chlorite (oversampled)	9.9159	8.4540
Chlorite (undersampled)	4.6475	3.1206
Pyroxene	1.1960	-0.5045
Vesuvianite	8.0894	6.1390

Table 1. The SNR increases of two denoising methods averaged across SNR levels of 20, 30 and 40, per signal

Using the test data set created along with the training data set as artificially constructed data, a target detection map was obtained for each of the seven targets. The discrete l^2 error of the maps (defined as the l^2 norm of the difference between the map and the known abundance of the artificial data) was measured for each pixel, and the mean error and standard deviation were taken across the image for three possible analysis methods; no analysis, wavelet analysis and wavelet analysis with denoising. These results are shown in table 2. It can be seen in this case that wavelet analysis has lead to a lower mean error and smaller standard deviation. However, denoising has not improved the results. This inconsistency is carried through to the unmixed data, in table 3. However, it can be seen that the unmixing process has yielded much lower errors, and extremely small mean least-squares errors between the actual spectra and the spectra constructed from the unmixing.

Analysis Type	Mean Error	Standard Deviation
None	0.3996	0.1702
Wavelet	0.3210	0.1560
Denoising	0.3346	0.1640

Table 2. Mean error and standard deviation of the target detection multistage method when run on artificial data

Analysis Type	Mean Error	Standard Deviation	Mean LS error
None	0.2778	0.2140	0.0003
Wavelet	0.2199	0.1926	0.0003
Denoising	0.2395	0.2023	0.0003

Table 3. Mean error, standard deviation and mean least-squares error of the unmixing method when run on artificial data

When the unmixing method is run on a real core image, we do not know the actual abundances and can thus only measure the LS error between the unmixed spectra and the actual spectra. These results are shown in table 4. In this case, we see rather poor performance from the wavelet analysis method (when compared to the other two methods). While the mean error of the wavelet denoised data is slightly higher than that of the unanalysed data, we see that, across the core, the denoised data has a lower standard deviation, indicative of tighter bounds on the error. Further tests will have to be conducted before any conclusions can be drawn about the efficacy of the analysis method. From a geological standpoint, we can see that the results obtained are sensible, as is shown in figure 1. Quartz (shown in green) appears in discrete pebbles bearing intrusion features, while chlorite (in red) and sericite (in blue) are mixed in places. The other targets are omitted from this diagram.

Analysis Type	Mean LS Error	Standard Deviation
None	0.0019	0.0312
Wavelet	0.0059	0.0668
Denoising	0.0021	0.0245

Table 4. Mean LS error and standard deviation between spectra reconstructed from unmixed abundances and real core spectra

4. CONCLUSION

A supervised multistage method for the automatic detection of multiple target minerals in hyperspectral mineral data was presented in

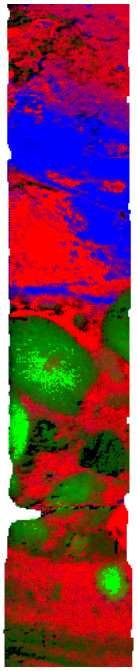

Fig. 1. A section of unmixed core showing sericite in blue, chlorite in red and quartz in green.

this paper. The method relies on wavelet analysis and wavelet-based denoising using thresholds. Fuzzy ROC curves were used to find a feature subset of maximal discrimination, in order to reduce the high dimensionality of the wavelet data. The processing step is fully decoupled, allowing limitless parallelisation in the spatial domain. A post-processing step was also presented, which produces abundance ratios of each target mineral, subject to nonnegativity and sum-to-one constraints.

It can be seen from the figure that the technique discussed in this paper produces good results in practice for the HCI. As yet, it is unclear whether wavelet analysis and denoising generally produces better results than other established methods. However, our method results in low least-squares errors. At the time of writing, further work was being performed to test our method against other target detection and unmixing methods in the context of this application.

5. REFERENCES

[1] Kerry-Anne Cawse, Steven Damelin, Louis du Plessis, Richard McIntyre, Michael Mitchley, and Michael Sears, "An investigation of data compression techniques for hyperspectral core imager data," in *Proceedings of the Mathemathics in Industry Study Group*, 2008, pp. 1–25.

[2] L.M. Bruce, C.H. Koger, and Li Jiang, "Dimensionality reduction of hyperspectral data using discrete wavelet transform feature extraction," *IEEE Transactions on Geoscience and Remote Sensing*, vol. 40, pp. 2331–2338, Oct. 2002.

[3] Cliff H. Koger, Lori M. Bruce, David R. Shaw, and Krishna N. Reddy, "Wavelet analysis of hyperspectral reflectance data for detecting pitted morning glory (ipomoea lacunosa) in soybean (glycine max)," *Remote sensing of environment*, vol. 86, pp. 108–119, 2003.

[4] Pieter Kempeneers, Steve De Backer, Walter Debruyn, and Paul Scheunders, "Wavelet based feature extraction for hyperspectral vegetation monitoring," in *Proceedings of the Image and Signal Processing for Remote Sensing IX*, 2004, vol. 5238, pp. 297–305.

[5] I. Daubechies, *Ten Lectures on Wavelets*, SIAM, 1992.

[6] James E. Fowler and Justin T. Rucker, "Three-dimensional wavelet-based compression of hyperspectral imagery," in *Hyperspectral Data Exploitation: Theory and Applications*, Chein-I Chang, Ed., pp. 379–407. Wiley-Interscience, 2007.

[7] Xiaoli Tang and William A. Pearlman, "Three-dimensional wavelet-based compression of hyperspectral images," in *Hyperspectral Data Compression*, Giovanni Motta, Francesco Rizzo, and James A. Storer, Eds., pp. 273–308. Springer, 2006.

[8] Lori M. Bruce, Cliff Morgan, and Sara Larsen, "Automated detection of subpixel hyperspectral targets with continuous and discrete wavelet transforms," *International Journal of Remote Sensing*, vol. 39, pp. 2217–2226, 2001.

[9] Frederic Schmidt, Sylvain Doute, and Bernard Schmitt, "Wavanglet: An efficient supervised classifier for hyperspectral images," *IEEE Transactions on Geoscience and Remote Sensing*, vol. 45, pp. 1374–1385, May 2007.

[10] Sinthop Kaewpijit, Jacqueline Le Moigne, and Tarek El-Ghazawi, "Automatic reduction of hyperspectral imagery using wavelet spectral analysis," *IEEE Transactions on Geoscience and Remote Sensing*, vol. 41, pp. 863– 871, April 2003.

[11] David L. Donoho, "De-noising by soft-thresholding," *IEEE Transactions on Information Theory*, vol. 41, pp. 613–627, 1995.

[12] United States Geological Society, "Usgs digital spectral library," http://speclab.cr.usgs.gov/spectral-lib.html, 2008, Last accessed 22 November 2008.

[13] David L. Donoho and Iain M. Johnstone, "Adapting to unknown smoothness via wavelet shrinkage," *Journal of the American Statistical Association*, vol. 90, no. 432, pp. 1200–1225, 1995.